POLITECNICO DI TORINO
Repository ISTITUZIONALE

Prediction of carotid restenosis risk after endarterectomy by hemodynamic and geometric analysis: a 5-years follow up

Original
Prediction of carotid restenosis risk after endarterectomy by hemodynamic and geometric analysis: a 5-years follow up / Gallo, Diego; Domanin, Maurizio; Vergara, Christian; Morbiducci, Umberto. - ELETTRONICO. - (2019). (2019 Summer Biomechanics, Bioengineering, and Biotransport Conference (SB3C2019) Seven Springs (USA) June 25-28, 2019).

Availability:
This version is available at: 11583/2743613 since: 2019-07-26T11:02:39Z

Publisher:
SB3C Foundation

Published
DOI:

Terms of use:

This article is made available under terms and conditions as specified in the corresponding bibliographic description in the repository

Publisher copyright

(Article begins on next page)

07 May 2026

SB^{3}C2019
Summer Biomechanics, Bioengineering and Biotransport Conference
June 25 -28, Seven Springs, PA, USA

PREDICTION OF CAROTID RESTENOSIS RISK AFTER ENDARTERECTOMY BY HEMODYNAMIC AND GEOMETRIC ANALYSIS: A 5-YEARS FOLLOW-UP

Diego Gallo (1), Maurizio Domanin (2), Christian Vergara (3), Umberto Morbiducci (1)

(1) Polito^{BIO}Med Lab, Department of Mechanical and Aerospace Engineering
Politecnico di Torino
Turin, Italy

(2) Department of Clinical Sciences and Community Health
Università di Milano
Milan, Italy

(3) Laboratory of Biological Structure Mechanics (LaBS), Department of Chemistry, Materials and Chemical Engineering "Giulio Natta"
Politecnico di Milano
Milan, Italy

INTRODUCTION

Restenosis is the main complication affecting patients outcome after carotid endarterectomy (CEA) [1]. The evidence that late (>5 years) restenosis is similar to primary atherosclerotic lesions [1], for which a key role of low and oscillatory wall shear stress (WSS) is established [2], has led to identify in local hemodynamic disturbances a possible contributor to the development of late restenosis after CEA. Additionally, the clinical translation of the role of hemodynamic disturbances in vascular pathology have motivated the identification of specific geometric attributes of the carotid bifurcation as surrogate markers of the burden of low and oscillatory WSS [3].

The elucidation of the mechanistic processes underlying restenosis development would greatly help clinical decision making about the appropriate CEA closure technique. Clinical debate currently exists concerning closure based on a direct suture (primary closure, PC), or on the interposition of a synthetic graft (patch graft, PG) [4]. To minimize the risk of narrowing of the arterial lumen, the use of PG is recommended for routine use by current guidelines [5]. However, PG involves longer cross-clamping time, higher risk of neurocognitive deficits, infection, pseudoaneurysm development. A selective use for PG based on carotid diameters has also been suggested [4, 5].

Here we aim to establish whether hemodynamics and geometry post-CEA can predict the risk of late restenosis at 5 years in a cohort of 12 real world patients submitted to 13 CEA with two different closure techniques (9 PG, 4 PC). In detail, personalized computational fluid dynamics (CFD) simulations and a geometric analysis were performed and compared with clinical follow up data of intima-media thickness (IMT) at 5 years, to investigate the hemodynamics-driven processes underlying restenosis development and potentially guiding the PG *vs.* PC clinical decision.

METHODS

The study was approved by the I.R.C.C.S. Fondazione Policlinico Ethics Committee and patients provided informed consent.

Patient population data. 13 carotid endarterectomy procedures were performed in 12 asymptomatic patients with diameter stenosis >70%, as defined by a peak systolic velocity (PSV) >200 cm/s measured by Doppler Ultrasound (DUS). According to European guidelines [5], PG angioplasty was performed in 9 cases (PG1-9), PC in 4 cases (PC1-4). All patients were submitted to DUS follow-up at 3 months, 2 and 5 years. Cases with PSV >130 cm/s (indicating a diameter stenosis >50%) were defined as cases of restenosis. No patients presented restenosis at 3 months and 2 years follow ups. Two patients died for myocardial infarction (PG4), and pancreatic carcinoma (PG8) at 3 years. After 5 years, eligible patients were submitted to DUS follow-up for IMT measurements with linear 8 MHz probe and iU22 ultrasound scanner (Philips Ultrasound, USA). IMT values were automatically extracted with Qlab (Philips Ultrasound, USA) at these locations: internal carotid artery (ICA) distal to the carotid bulb (CB); CB; distal end of the common carotid artery (CCA), i.e., the flow divider (FD); CCA at 1 and 2 cm below the flow divider (FD-1cm and FD-2cm, respectively).

Computational hemodynamics. MRI acquisitions (Siemens 1.5T Avanto) were performed within 1 month after surgery and used for 3D geometry reconstruction [6]. The governing equations of fluid motion were solved using P1 bubble-P1 tetrahedral finite elements in the library LifeV (http://www.lifev.org). Patient-specific flow rate waveforms were extracted from echo-color DUS at the CCA and ICA and imposed as boundary conditions [6]. At the external carotid artery (ECA) outlet section, a traction-free condition was imposed [6]. The distributions at the luminal surface of time-averaged WSS (TAWSS), and oscillatory shear index (OSI) were calculated. The bifurcation

region was delimited by sections CCA3, ICA5 and ECA2 (Fig. 1A). Data from all 13 models were pooled to identify the 20th percentile value of TAWSS, and 80th percentile values of OSI. The burden of disturbed WSS was quantified by the surface area exposed to TAWSS, below (OSI above) the corresponding threshold value, and divided by the model surface area [2]. These hemodynamic descriptors are denoted Low Shear Area (LSA) and Oscillatory Shear Area (OSA).

Geometric analysis. Descriptors quantifying the expansion at the bulb (i.e., flare), and the tortuosity of the CCA were considered [3]. Flare was calculated as the ratio between the maximum CCA cross-sectional area (CCA_{max}) and the CCA3 area (Fig. 1A). Tortuosity was calculated between the "inflection point", i.e. the point where the CCA-ICA centerline changes concavity, and the CCA3 centerline point (Fig. 1B) as Tort=L/D-1, where L and D are the curvilinear and Euclidean distance between the two points, respectively.

Statistical analysis. The relationship between the hemodynamic descriptors and the combination of geometric descriptors was quantified by multiple linear regression analysis. The quality of the regression was evaluated with the adjusted coefficient of determination R^2, and the relative contribution of each predictor was determined from the standardized regression coefficients β. Then, linear regression analysis was used to identify relationships between hemodynamic or geometric descriptors with maximum IMT values.

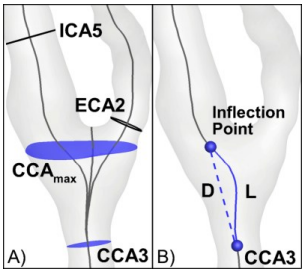

Figure 1: A) CCA_{max} and CCA3 sections, whose ratio defines the flare, are shown in blue. CCA_{max} is normal to the average of the ICA and ECA centerlines. B) The centerline segment between the CCA3 centerline point and the inflection point was used to calculate tortuosity as L/D -1.

RESULTS

Statistically significant differences were observed between the PG and PC groups for LSA and flare (P<0.05), but not OSA nor tortuosity. In detail, PG patients exhibited larger average values of LSA than PC patients (40.85%±19.10% *vs*. 19.42%±10.61%), and higher flare values (2.60±1.42 *vs*. 1.33±0.10). This is not unexpected, since the inserted PG substitutes a portion of the endarterectomized vessel wall which is removed in PC. Notwithstanding the small sample size, a direct relationship emerged between flare and LSA (P<0.05), but not OSA (Table 1). Linear regressions revealed direct associations between maximum IMT at 5 years and both LSA (R^2=0.58, P=0.006), and flare (R^2=0.74, P<0.001) (Fig. 2A), whereas maximum IMT was not correlated with either OSA (R^2=0.15, P=0.241), or tortuosity (R^2=0.25, P=0.116). At 5 years, DUS highlighted the presence of a >70% restenosis in PG1, and >50% restenosis in PG2 (right and left carotid in the same patient), confirmed by magnetic resonance angiography and intra-operatory arteriography (Fig. 2B,C). A clear co-localization emerged between the area exposed to low WSS and the restenosis location (Fig. 2D). This is further confirmed for all cases in Fig. 3, where morphological DUS observations, presented with TAWSS and OSI distributions, allow to appreciate by visual inspection the co-localization between disturbed hemodynamics and observations of myointimal thickening or new atheroma development.

Table 1: Multiple regression of geometry *vs*. hemodynamics.

	Adjusted R^2	β flare	β tortuosity
LSA	0.359*	0.743*	-0.255
OSA	0.132	0.574	-0.200

* P<0.05

DISCUSSION

While the mechanisms leading to restenosis after CEA are still being defined, the establishment of flow disturbances at the bifurcation has been often interpreted by surgeons as an harbinger of complications [4,5]. Here, we successfully linked disturbed hemodynamics after CEA to verified clinical cases of late restenosis, additionally exploring the clinical translation of such a link through surrogate geometric predictors of disturbed hemodynamics. These findings imply that the arteriotomy after CEA should avoid creating a large and sudden expansion, as it is linked to restenosis via the generation of flow disturbances. This is particularly true in obliged PG arteriotomy repair strategies. Our findings suggest also that hemodynamic and geometric analyses hold potential for the stratification of patients at risk for development of late restenosis, providing useful indications about (1) the best arteriotomy repair strategy, and (2) the best follow up strategy. In particular, geometric analysis could be easily integrated in a surgical planning pipeline to virtually explore personalized post-operative scenarios.

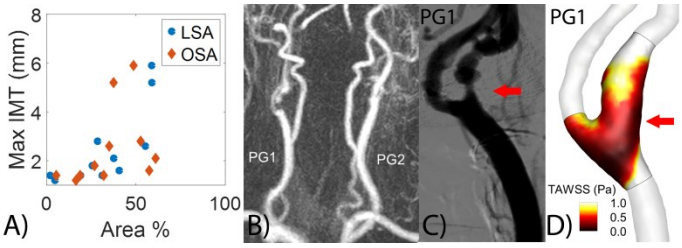

Figure 2: A) Scatter plots of LSA and OSA *vs*. maximum IMT. B), C) Clinical evidence of restenosis for PG1 and PG2. D) The restenosis region was characterized by low WSS (red arrow).

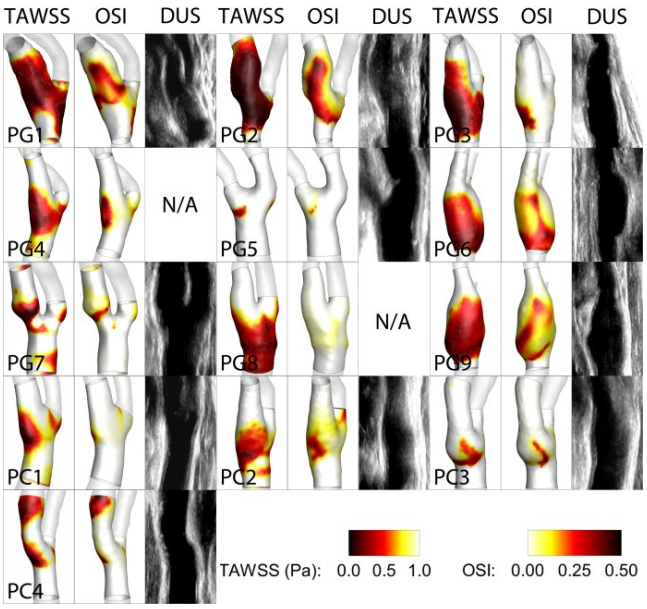

Figure 3: Contour maps of TAWSS and OSI with DUS images at 5 years follow up, showing carotid IMT.

REFERENCES

[1] Hellings, WE et al., *Stroke*, 39:1029-1032, 2008.
[2] Gallo, D et al., *J R Soc Interface*, 15: 20180352, 2018.
[3] Bijari, PB et al., *J Biomech*, 45: 1632-1637, 2012.
[4] Kumar, R et al., *Eur J Vasc Endovasc Surg*, 53(6):776-775, 2017.
[5] Naylor, AR et al., *Eur J Vasc Endovasc Surg*, 55(1):3-81, 2017.
[6] Guerciotti, B et al., *J Biomech*, 49:26-38, 2016.